

# Molecular-size-distribution-dependent aggregation of humic substances by Na(I), Ag(I), Ca(II), and Eu(III)

メタデータ	言語: eng 出版者: 公開日: 2017-10-05 キーワード (Ja): キーワード (En): 作成者: メールアドレス: 所属:
URL	<a href="https://doi.org/10.24517/00029340">https://doi.org/10.24517/00029340</a>

This work is licensed under a Creative Commons Attribution-NonCommercial-ShareAlike 3.0 International License.



# Molecular-size-distribution-dependent aggregation of humic substances by Na(I), Ag(I), Ca(II), and Eu(III)

Shuji Tamamura <sup>a,\*</sup>, Ryutaro Ohashi <sup>b</sup>, Seiya Nagao <sup>a</sup>, Masayoshi Yamamoto <sup>a</sup>, Motohiro Mizuno <sup>b</sup>

<sup>a</sup> Low Level Radioactivity Laboratory, INET, Kanazawa University, Wake, Nomi, Ishikawa 923-1224, Japan

<sup>b</sup>Theoretical Chemistry Laboratory, INET, Kanazawa University, Kakuma, Kanazawa, Ishikawa 920-1192, Japan

\* Corresponding author. Present address: 5-3 Sakae-machi, Horonobe-cho, Teshio-gun, Hokkaido 098-3221, Japan. Tel: +81-1632-9-4112; Fax: +81-1632-9-4113; E-mail: shuji-tamamura@h-rise.jp

Author e-mail addresses:

Shuji Tamamura: shuji-tamamura@h-rise.jp

Seiya Nagao: s\_nagao@llrl.ku-unet.ocn.ne.jp

Masayoshi Yamamoto: pluto@llrl.ku-unet.ocn.ne.jp

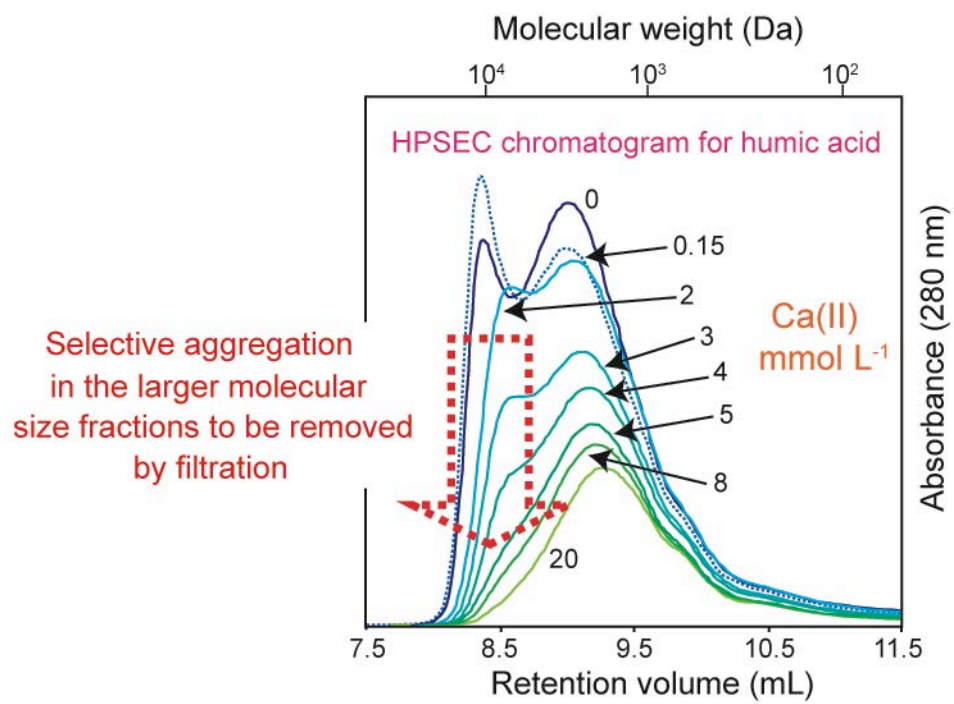
Ryutaro Ohashi: ryu@wiron1.s.kanazawa-u.ac.jp

Motohiro Mizuno: mizuno@se.kanazawa-u.ac.jp

## **Highlights**

- >Molecular-size-distribution (MSD)-dependent aggregation of humics was investigated.
- >Larger molecular size fractions selectively coagulated by Na and Ca.
- >The MSD dependence was attributed to non-specific binding of Na and Ca to humics.
- >Large and small molecular size fractions concurrently coagulated by Ag and Eu.
- >The reduced MSD dependence was caused by specific binding of Ag and Eu to humics.

## Graphical Abstract



## **ABSTRACT**

Molecular-size-distribution (MSD)-dependent aggregation of Fluka and International Humic Substance Society humic acids (HAs) in the presence of Na(I), Ca(II), Ag(I), and Eu(III) were studied using high-performance size-exclusion chromatography. Larger molecular size fractions (>8000 Da) rich in aliphatic carbons were observed to aggregate in the presence of Na(I) and Ca(II), whereas both large and small molecular size fractions concurrently aggregated in the presence of Ag(I) and Eu(III). In view of the non-specific binding of Na(I) and Ca(II) with HAs, the electric-field screening effect is probably the main cause of HA aggregation by Na(I) and Ca(II), preserving the intrinsic hydrophobicity of the HAs. Reduced surface charges and the hydrophobic heterogeneities of different MSD fractions of HAs by direct binding of Ag(I) and Eu(III) are postulated to induce insignificant dependence of aggregation on the different MSD fractions.

*Keywords:* Humic acid; molecular size distribution; aggregation; high-performance size-exclusion chromatography; <sup>13</sup>C NMR.

## 1. Introduction

Humic substances (HS) are the most abundant heterogeneous organic matter found in surface environments [1]. Such substances are classified into soluble fulvic acids (FA) and insoluble humic acids (HA) at pH values less than one, and insoluble humin at any pH value. In aquatic environments, FA and HA aggregate in response to increases in ion concentrations [2–7], thereby affecting the toxic metal migration associated with HS. The molecular weights of HA range from 500 to 20 000 Da [8–13], and this may induce molecular-size-distribution (MSD)-dependent aggregation of HA as a result of the rise in ion concentrations. Currently, only a handful of limited studies have been performed on this topic (e.g., [4,14,15]).

In this context, we focused on the occurrence and extent of MSD-dependent aggregation of HA, using high-performance size-exclusion chromatography (HPSEC). Na(I) and Ca(II) were used to induce HA aggregation because both ions are commonly found in natural waters. Eu(III) was included as a metal ion with a relatively high stability constant [16,17] with HA. Ag(I) was included as a “soft” monovalent ion that strongly binds to HA compared to a “hard” monovalent ion such as Na(I) [18]. The chemical structures of the aggregates (trapped on 0.45- $\mu\text{m}$  filters) and non-aggregated (filtered) fractions were also examined using  $^{13}\text{C}$  NMR. For comparison, two kinds of HA were employed in this study.

## 2. Material and methods

### 2.1. Aggregation experiments

Fluka HA and Peat HA were purchased from the Fluka Chemical Corp. (Milwaukee, WI, USA) and International Humic Substance Society (IHSS), respectively. The ash and acid functional group contents are summarized in Table 1. Stock solutions were prepared by dissolving 12.5 mg of each HA in 0.1 mol L<sup>-1</sup> NaOH. After stirring the solutions overnight, the pH values were adjusted to a neutral value by adding 0.1 mol L<sup>-1</sup> HClO<sub>4</sub> and NaOH. The solution volumes were fixed at 25 mL using volumetric flasks after filtration through 0.45- $\mu\text{m}$  filters to reduce the ash contents of the HAs [19]. The removed HAs by the filtration was negligible, as estimated from the total organic carbon (TOC) concentrations before and after the filtration. Stock solutions of 3.5 mol L<sup>-1</sup> Na(I), 0.3 mol L<sup>-1</sup> Ag(I), 0.5 mol L<sup>-1</sup> Ca(II), and 1–10 mmol L<sup>-1</sup> Eu(III) were prepared by dissolving sodium chloride, silver perchlorate monohydrate,

calcium chloride, and europium nitrate hexahydrate, respectively. The pH values of these solutions were adjusted to slightly acidic values by adding minute amounts of 1 mol L<sup>-1</sup> HCl, 0.1 mol L<sup>-1</sup> HNO<sub>3</sub>, or 0.1 mol L<sup>-1</sup> HClO<sub>4</sub>. All chemical compounds were purchased from Wako Pure Chemical Industries, Ltd. (Osaka, Japan), as guaranteed reagent grade.

Using the stock solutions, 50 mg L<sup>-1</sup> of the HA solutions in the presence of Na(I) (0–3.5 mol L<sup>-1</sup>), Ag(I) (0–20 mmol L<sup>-1</sup>), Ca(II) (0–20 mmol L<sup>-1</sup>), and Eu(III) (0–70 μmol L<sup>-1</sup>), respectively, were prepared without adding supporting electrolytes. The pH values of the samples were adjusted to slightly acidic to neutral by adding predetermined volumes of 1 mmol L<sup>-1</sup> HClO<sub>4</sub>. After shaking the samples overnight at 25 °C in the dark using a shaking apparatus with automatic temperature adjustment, the solutions were filtered through 0.45-μm filters to remove aggregated HA fractions, and stored for subsequent pH and HPSEC analyses.

## 2.2. HPSEC

The HPSEC system consisted of a Hitachi model L-6000 pump (Hitachi, Tokyo, Japan), an L-5020 column oven (kept at 30 °C), a Rheodyne 7125 injection valve with a 20-μL sample loop, and a Hitachi model L-2420 UV-Vis detector. The separation was performed using a stainless-steel gel-permeation chromatography (GPC) column (Hitachi GL-W530: 30 cm × 10.7 mm ID) packed with a water-soluble polyacrylate gel resin. A guard column packed with the same materials (5 cm × 10.7 mm ID) was used to protect the GPC column. According to the manufacturer's specifications, the approximate upper exclusion limit was 50 000 Da (calibrated with pullulan). The specific interaction of HA with the column (ionic expulsion and specific adsorption [12]) was minimized by the flow of a proper mobile phase (0.01 mol L<sup>-1</sup> Tris-HCl buffer at pH 8.0 in a 0.01 mol L<sup>-1</sup> NaCl solution [11]) at the flow rate of 1 mL min<sup>-1</sup>. The recovery of the HA through the column was more than 75%, as determined by comparing the total UV (280 nm) peak areas for the HA samples passing through and bypassing the column.

Polystyrene sulfonate sodium salts are rather preferable standards for molecular weight calibration of HS [9,12,20], and were used in this study. The selected molecular weights for the calibration were 1100, 3610, 6530, 14 900, and 32 900 Da. The void and total volumes of the column were 8.4 mL and 23.6 mL, as determined using blue dextran and acetone, respectively.

The phenolic arenes, benzoic acids, aniline derivatives, and polycyclic aromatic

hydrocarbons with two or more benzene rings are thought to be common structural units in HS [9], which have high molar absorption coefficients in the UV region (ca. 270–280 nm). In this context, the wavelength for the UV-Vis detector was set at 280 nm for all the samples [8,9]. The chromatogram measurements were performed in duplicate.

### 2.3. $^{13}\text{C}$ NMR

Chemical structural differences between the aggregated and non-aggregated fractions in the presence of the metal ions were investigated by  $^{13}\text{C}$  NMR using Fluka HA. The reaction of 1.0 g L<sup>-1</sup> Fluka HA solutions with Na(I), Ca(II), and Eu(III) were carried out at the concentrations of 3.5 mol L<sup>-1</sup>, 4.0 mmol L<sup>-1</sup>, and 1.22 mmol L<sup>-1</sup>, respectively. For the Ag(I) experiment, 0.1 g L<sup>-1</sup> Fluka HA solution was reacted with Ag(I) at the concentration of 12.3 mmol L<sup>-1</sup>. The high HA concentration (0.1–1.0 g L<sup>-1</sup>) was used to collect sufficient amounts of aggregated and non-aggregated HA for the  $^{13}\text{C}$  NMR spectral measurements. The trapped (aggregated) fractions on the filter and filtered (non-aggregated) fractions were dialyzed, and subsequently freeze-dried. Typically, more than 95% of the used HA in the reaction was recovered in the freeze-dry processes, as estimated from the combined weight of the aggregated and non-aggregated HA. The percentages of the aggregated HA were 76%, 86%, 18%, and 53% for the Na(I), Ca(II), Eu(III), and Ag(I) experiments, respectively. In addition to the aggregated and non-aggregated HA, the  $^{13}\text{C}$  NMR spectrum of the Fluka HA itself was also measured.

All solid-state NMR experiments were carried out at 6.9 T (74.18 MHz for  $^{13}\text{C}$ ) using a JEOL ECA-300 NMR spectrometer and a JEOL 4.0 mm CP-MAS probe. All samples were spun at 14 kHz and at 298 K. At this spinning rate, the temperatures in all sample rotors were calibrated at 324 K by  $^{207}\text{Pb}$  NMR experiments on  $\text{Pb}(\text{NO}_3)_2$  [21]. The  $^{13}\text{C}$  chemical shifts were calibrated in ppm relative to TMS by taking the  $^{13}\text{C}$  chemical shift for the methane  $^{13}\text{C}$  of solid adamantane (29.5 ppm) as an external reference standard. For the  $^{13}\text{C}$  1D spectra, the echo technique developed by Kunwar et al. [22] was applied using the following condition: total echo time = 71.4  $\mu\text{s}$ , relaxation delay = 4.0 s, number of scans = 32 000 (Fluka HA, Na(I) aggregated, Na(I) filtered, Ca(II) aggregated, Eu(III) filtered) or 64 000 (Ca(II) filtered, Eu(III) aggregated, Ag(I) aggregated, Ag(I) filtered), and  $^1\text{H}$  decoupling power = 120 kHz with the TPPM technique [23]. All spectra were broadened with a single-exponential function at 20 Hz. A small amount of samples were placed between two silicon-rubber spacers (1.5 ppm).

### 3. Results

#### 3.1. Absorbances

Free metal ions in the solutions should have been present in the forms of  $\text{Na}^+$  (pH 5–6),  $\text{Ag}^+$  (pH 6–7),  $\text{Ca}^{2+}$  (pH 6.5–7.5), and  $\text{Eu}^{3+}$  (pH 5–6) at the measured pH ranges used (Geochemical Work Bench 7.0, RockWare, Golden, USA). In the presence of Na(I), the absorbances of both HAs gradually decreased as the concentration of Na(I) increased (Fig. 1a). At the maximum concentration ( $3.5 \text{ mol L}^{-1}$ ), the remaining absorbance values for the Fluka and IHSS HAs were about 40% and 60%, respectively. In the case of Ca(II), the absorbances of both HAs decreased slightly up to  $3 \text{ mmol L}^{-1}$  of Ca(II), followed by a sharp decline in absorbance values above this concentration (Fig. 1c). The remaining absorbance values were 34% and 33% for the Fluka and IHSS HAs, respectively, at the maximum Ca(II) concentration ( $20 \text{ mmol L}^{-1}$ ).

Absorbance values for Ag(I) and Eu(III) (Figs. 1b and 1d, respectively) remained fairly stable up to certain metal concentrations, followed by sharp declines above particular concentrations. The critical concentrations for the Fluka and IHSS HAs, respectively, were 9 and  $11 \text{ mmol L}^{-1}$  for Ag(I), and  $40$  and  $45 \text{ }\mu\text{mol L}^{-1}$  for Eu(III). The critical concentrations for Fluka HA were always lower than the values obtained for IHSS HA.

#### 3.2. HPSEC chromatograms

Figs. 2 and 3 show changes in the HPSEC chromatograms as the concentration of the metal ions increased in the Fluka and IHSS HA samples. In the absence of metal ions, the chromatograms of both HAs had two peaks, at retention volumes of 8.4 mL (peak 1) and  $\sim 9$  mL (peak 2), i.e., in the molecular-weight ranges  $>8000$  Da and  $1000$ – $8000$  Da. As shown in Figs. 2 and 3, the chromatograms changed in a similar manner for both the Fluka and IHSS HAs for a given metal ion. A clear preferred reduction in the peak area at lower retention volumes (corresponding to peak 1) was a distinct feature in the presence of Na(I) and Ca(II), along with an increase in Na(I) and Ca(II) concentrations (Figs. 2a, 2c, and 3a, 3c). The preferred reduction is expected to reflect the selective aggregation of larger molecular size fractions to be removed by filtration. Such selective aggregations of HS species in the presence of Na(I) and Ca(II) have been noted previously [4,14]. Contrastively, both peaks 1 and 2 were concurrently reduced with an increase in Ag(I) and Eu(III) concentrations (Figs. 2b, 2d and 3b, 3d).

Fig. 4 shows the peak height ratios of peak 1 to peak 2 (peak 1/peak 2) as a function of metal ion concentrations. For the chromatograms where peak 1 was significantly attenuated and no longer detectable, chromatogram intensities at the retention volume of 8.4 mL were used. The peak height ratios decreased rapidly compared with the absorbance values as a result of increases in the concentration of Na(I) (Fig. 4a). For example, the observed decreases in the percentages of the peak height ratios for both HAs were about 90%, whereas the absorbance decreases were about 40% for Fluka HA, and 60% for IHSS HA at 3.5 mol L<sup>-1</sup> Na(I). In the case of Ca(II), the peak height ratios and absorbance values decreased similarly (within 10% difference) as the concentration of Ca(II) increased from 2.0 to 20 mmol L<sup>-1</sup> (Fig. 4c).

In contrast to the results obtained with Na(I) and Ca(II), the peak height ratios remained fairly stable, compared with a significant reduction in the corresponding absorbance values, when examining Ag(I) and Eu(III) (Figs. 4b and 4d, respectively). For example, 75% reductions in the Fluka and IHSS HA absorbance values were observed for Ag(I) concentrations of 11 and 14 mmol L<sup>-1</sup>, respectively; however, only 5% and 20% reductions in the corresponding peak height ratios were measured (Fig. 4b). Reductions of more than 80% and 70% in absorbances at Eu(III) concentrations of 42 and 50 μmol L<sup>-1</sup> for the Fluka and IHSS HAs, respectively, were accompanied by 5% and <20% reductions in the corresponding peak height ratios (Fig. 4d). These stable features of the peak height ratios are indicated by vertical arrows in Figs. 4b and 4d, respectively.

Further increases in the Ag(I) and Eu(III) concentrations beyond their critical concentrations, however, caused significant peak height ratio reductions in both HAs. The ratios decreased by about 60% at Ag(I) concentrations of 14 and 18 mmol L<sup>-1</sup> for the Fluka and IHSS HAs, respectively (Fig. 4b). In the presence of Eu(III), the peak height ratios decreased by 90% for Fluka HA and ~70% for IHSS HA at concentrations of 50 and 70 μmol L<sup>-1</sup> of Eu(III), respectively (Fig. 4d). The peak height ratio reductions reflect selective aggregation of larger molecular size fractions.

In the initial stages of HA aggregation, where the absorbance reduction was <30% of the original absorbance, the peak height ratios were found to increase (by up to 30%) as the Na(I), Ca(II), and Eu(III) concentrations increased. These features are indicated by oblique arrows in Figs. 4a, 4c, and 4d. The enhancements in the peak height ratios indicate selective aggregation of smaller molecular size fractions during the initial stages of HA aggregation.

### 3.3. <sup>13</sup>C NMR spectra

In the  $^{13}\text{C}$  NMR spectrum of Fluka HA (Fig. 5a), two strong peaks appeared between 30 and 40 ppm, and weaker peaks appeared at ~17 and 26 ppm. These peaks are assigned to methane, methylene, or methyl carbons, and are sharper than all the other peaks in the  $^{13}\text{C}$  NMR spectra. These sharp peaks indicate that Fluka HA have a significant amount of homogeneous structures containing aliphatic carbons, because heterogeneous structures broaden the  $^{13}\text{C}$  peaks.

In the presence of Na(I) and Ca(II), the peaks for aliphatic carbon (5–60 ppm) were evident in the aggregated HA (Figs. 5b and 5f, respectively) but not evident in the non-aggregated HA (Figs. 5c and 5g, respectively). Contrastively, the spectral shape of aggregated and non-aggregated HA were similar to each other in the presence of Ag(I) or Eu(III) (as can be seen by comparing Figs. 5d and 5e, or Figs. 5h and 5i, respectively).

The spectral features for the aggregated HA strongly depended on the associated metal ions. In particular, the strong peaks between 30 and 40 ppm in Na(I)-aggregated HA were attenuated, especially in Ag(I) and Eu(III)-aggregated HA. The portion of aromatic carbon (110–165 ppm) in the Ca(II)-aggregated HA was relatively enhanced, while that of acetal carbon (92–110 ppm) became prominent in the Ag(I) and Eu(III)-aggregated HA. The spectra for non-aggregated HA were also different from each other.

The  $^{13}\text{C}$  NMR spectrum of an organic molecule can be altered upon complexation of metal ions owing to distortion of electrical charge density of the molecule, affecting  $^{13}\text{C}$  nuclear magnetic shielding [24–27]. The HA spectral dependence on the present metal ions indicate different manner of interaction between HA and the metal ions. The similarity of the spectrum of Na(I)-aggregated HA to that of Fluka HA itself would imply the weakest interaction of Na(I) with HA.

## 4. Discussion

### 4.1. Electric-field screening

Ong and Bisque [2] suggested the DLVO (Derjaguin–Landau–Verwey–Overbeek) theory [28,29] as the mechanism of humic colloidal aggregation. In this theory, colloidal stability is determined by two competing forces between colloids: Van der Waals–London attractions and electrical repulsions. Since the attractive force is independent of the solution conditions, it is the electrical

repulsions that are reduced as the ion concentration increases. Both surface charge reduction by bound ions on the surface and electric-field screening can reduce the electrical repulsion. The latter effect is quantified by the Debye length ( $r_A$ ). This is the length perpendicular to the colloidal surface where the electric potential decreases by more than 60% of the surface electric potential [28,29]. The Debye length is formulated as

$$\Gamma_A = \left( \frac{\sum_i \rho_i e^2 z_i^2}{\varepsilon \varepsilon_0 k T} \right)^{-\frac{1}{2}} \quad (1)$$

where  $\rho_i$  is the concentration of ion “i” ( $\text{m}^{-3}$ ),  $e$  is the charge on an electron (C),  $z_i$  is the valence of ion “i,”  $\varepsilon$  is the dielectric constant of water,  $\varepsilon_0$  is the permittivity of a vacuum ( $\text{C}^2 \text{N}^{-1} \text{m}^{-2}$ ),  $k$  is the Boltzmann constant ( $\text{J K}^{-1}$ ), and  $T$  is the absolute temperature (K). The Debye length decreases as the ionic concentrations and valences increase. Shorter Debye lengths enable colloids to approach each other, leading to aggregation.

If the electric-field screening effect is the dominant cause of HA aggregation in the presence of the studied metal ions, the Debye lengths should be very similar when the solution conditions favor substantial aggregation, regardless of the metal ion type. Table 2 shows the Debye lengths when the solution conditions reduced the absorbance values by nearly half the values observed under the initial conditions. In the calculations, metal ions were assumed to be in free states, without binding to HA. The Debye lengths were 0.16–0.22 nm for Na(I), 2.68–2.91 nm for Ag(I), 2.28–2.50 nm for Ca(II), and 17.6–19.2 nm for Eu(III). The marked differences suggest that the electric-field screening effect cannot be the only cause of HA aggregation. Humic colloidal surface charge reduction by the binding of metal ions must also be considered [6].

#### 4.2. MSD-dependent aggregation

As the colloidal size increases, the electric charge for a colloidal particle also increases, assuming a constant charge density of the colloid. The electrical repulsion energies between large colloids should therefore be higher than those for smaller ones. In contrast, the colloidal kinetic energy is a function of only temperature and is independent of colloidal size. Smaller colloidal particles can therefore approach each other more easily, without the effects of strong electrical repulsion, resulting in aggregation [28]. The selective aggregation of smaller molecular size fractions, as

reflected by the enhancement in peak height ratios at the beginning of aggregation (oblique arrows in Figs. 4a, 4c, and 4d), may be explained by this mechanism.

At higher metal ion concentrations, however, selective aggregation of larger molecular size fractions was observed, especially in the presence of Na(I) and Ca(II) (Figs. 2a, 2c, and 3a, 3c). The  $^{13}\text{C}$  NMR spectra revealed that the aggregated fractions in the presence of Na(I) and Ca(II) were rich in aliphatic carbons (Figs. 5b and 5f, respectively). Enriched levels of aliphatic carbons in HA aggregates in the presence of Ca(II) were also observed by Christl and Kretzschmar [30] using C-1s near-edge X-ray absorption fine structure spectroscopy. Considering the hydrophobic character of aliphatic carbons [29], the enrichment of aliphatic carbons in the aggregates is reasonable because hydrophobic colloids can aggregate more readily than hydrophilic colloids, as a result of both hydrophobic interactions and hydrophilic repulsion effects [29]. We inferred that larger molecular size fractions of HA are enriched in aliphatic moieties [15,31,32] rendering hydrophobicity of the fractions, thus having a higher tendency to aggregate. The gradual decrease in the absorbance as a result of the increase in Na(I) and Ca(II) concentrations (Figs. 1a and 1c, respectively) would reflect gradual HA aggregations from hydrophobic large molecular size fractions to hydrophilic smaller ones.

In the moderate pH condition, the 1:1 binding constant ( $K$ ) of HA with metal ion is increased in the order of  $\text{Ca}^{2+}$  ( $\log K \approx 3.0$  for Aldrich HA [33])  $<$   $\text{Ag}^+$  ( $\log K \approx 4.0$  for lignite HA [34])  $<$   $\text{Eu}^{3+}$  ( $\log K \approx 6.0$  for Aldrich HA [16]). The affinity of Na(I) to HA should be lower than that of Ca(II), by considering the monovalent character of Na(I) ion ( $\text{Na}^+$ ). The higher affinity of  $\text{Ag}^+$  than that of  $\text{Na}^+$  is attributed to the “softness” of  $\text{Ag}^+$  in terms of the concept of hard and soft acids and bases (HSAB) theory [35]. The low affinity of Na(I) and Ca(II) corresponds to non-specific binding of these metal ions with HA [18,36]. Without direct binding to HA, Ca(II) and especially Na(I) should significantly reduce the electrical repulsion between HA colloids by the electric-field screening effect, preserving intrinsic hydrophobic heterogeneity of the HA.

In contrast, Ag(I) and Eu(III) directly bind with HA at their proton-exchange sites [18,36–38]. The direct binding of these ions with HA should reduce the surface charges of the HA [6], as expected from the longer Debye lengths, especially for Eu(III) (Table 2). The binding of these ions could also increase the hydrophobicity of the bound sites of HA [3,6,39,40]. Therefore, the insignificant dependence of aggregation on the different MSD fractions in the presence of Ag(I) and Eu(III) (Figs. 2b, 2d, and 3b, 3d) may be explained by the homogenized character of different MSD fractions in terms of

surface charge and hydrophobicity. This homogenization probably explains the observed sharp absorbance decrease in the Ag(I) and Eu(III) samples at their critical concentrations (Figs. 1b and 1d, respectively), signifying concurrent aggregation of different MSD fractions. The similarity of the  $^{13}\text{C}$  NMR spectra between aggregated and non-aggregated HA in the presence of Ag(I) or Eu(III) (as is evident from comparing Figs. 5d and 5e, or Figs. 5h and 5i, respectively) also indicated the reduced priority of the aliphatic moiety of HA for aggregation.

The decreasing trend in the peak height ratios at higher Ag(I) and Eu(III) concentrations compared with those observed for their corresponding critical concentrations (Figs. 4b and 4d, respectively) implies selective aggregation of larger molecular size fractions. This selective aggregation may have proceeded via the same mechanism as that observed for Na(I) and Ca(II), as discussed above. This observation is in agreement with the results of the work by Plaschke et al. [38]. This group used scanning transmission X-ray microscopy images and observed that some fractions in HA aggregates were enriched with aliphatic carbons in the presence of Eu(III).

## 5. Conclusion

MSD-dependent aggregations of both Fluka and IHSS HAs in the presence of Na(I), Ag(I), Ca(II), and Eu(III) were investigated. In the presence of Na(I) and Ca(II), larger molecular size fractions of HAs, rich in aliphatic carbons, were likely to aggregate, whereas both large and small molecular size fractions concurrently aggregated in the presence of Ag(I) and Eu(III). The marked differences were attributed to non-specific binding of Na(I) and Ca(II), and specific binding of Ag(I) and Eu(III) to the HAs. Non-specific binding would preserve the intrinsic hydrophobicity of the HAs, resulting in selective aggregation of the hydrophobic larger molecular size fractions. Specific binding of Ag(I) and Eu(III) to the HAs would homogenize the surface characteristics of the different MSD fractions in terms of surface charges and hydrophobicities, leading to insignificant dependence of aggregation on the different MSD fractions.

## **Acknowledgements**

The authors thank Dr. Syusaku Nishimura (Dept. of Chemistry, Kanazawa University) for his skilled technical assistance; Assistant Professor Keisuke Fukushi (Dept. of Earth Science, Kanazawa University) for his encouragement during the studies.

## References

- [1] F.J. Stevenson, *Humus Chemistry – Genesis, Composition, Reactions*, second ed., John Wiley & Sons, New York, 1994.
- [2] H.L. Ong, R.E. Bisque, Coagulation of humic colloids by metal ions, *Soil Sci.* 106 (1968) 220–224.
- [3] M. Yamamoto, M. Sakanoue, Interaction of humic acid and Am(III) in aqueous solution, *J. Radiat. Res.* 23 (1982) 261–271.
- [4] E. Tipping, M. Ohnstad, Aggregation of aquatic humic substances, *Chem. Geol.* 44 (1984) 349–357.
- [5] E. Balnois, K.J. Wilkinson, J.R. Lead, J. Buffle, Atomic force microscopy of humic substances: effects of pH and ionic strength, *Environ. Sci. Technol.* 33 (1999) 3911–3917.
- [6] N.D. Bryan, M.N. Jones, J. Birkett, F.R. Livens, Aggregation of humic substances by metal ions measured by ultracentrifugation, *Anal. Chim. Acta* 437 (2001) 291–308.
- [7] H. Lippold, A. Mansel, H. Kupsch, Influence of trivalent electrolytes on the humic colloid-borne transport of contaminant metals: competition and flocculation effects, *J. Contam. Hydrol.* 76 (2005) 337–352.
- [8] Y.-P. Chin, G. Aiken, E. O’Loughlin, Molecular weight, polydispersity, and spectroscopic properties of aquatic humic substances, *Environ. Sci. Technol.* 28 (1994) 1853–1858.
- [9] J. Peuravuori, K. Pihlaja, Molecular size distribution and spectroscopic properties of aquatic humic substances, *Anal. Chim. Acta* 337 (1997) 133–149.
- [10] R. Artinger, G. Buckau, J.I. Kim, S. Geyer, Characterization of groundwater humic and fulvic acids of different origin by GPC with UV/Vis and fluorescence detection, *Fresenius J. Anal. Chem.* 364 (1999) 737–745.
- [11] S. Nagao, T. Matsunaga, Y. Suzuki, T. Ueno, H. Amano, Characteristics of humic

substances in the Kuji river waters as determined by high-performance size exclusion chromatography with fluorescence detection, *Water Res.* 37 (2003) 4159–4170.

[12] I.V. Perminova, F.H. Frimmel, A.V. Kudryavtsev, N.A. Kulikova, G. Abbt-Braun, S. Hesse, V.S. Petrosyan, Molecular weight characteristics of humic substances from different environments as determined by size exclusion chromatography and their statistical evaluation, *Environ. Sci. Technol.* 37 (2003) 2477–2485.

[13] E.M. Perdue, J.D. Ritchie, Dissolved organic matter in freshwaters, in: J.I. Drever (Ed.), *Surface and Ground Water, Weathering, and Soils*, Elsevier, Oxford, 2005, pp. 273–318.

[14] E. Tombácz, Colloidal properties of humic acids and spontaneous changes of their colloidal state under variable solution conditions, *Soil Sci.* 164 (1999) 814–824.

[15] P. Conte, A. Piccolo, Conformational arrangement of dissolved humic substances. Influence of solution composition on association of humic molecules, *Environ. Sci. Technol.* 33 (1999) 1682–1690.

[16] T. Kubota, O. Tochiyama, K. Tanaka, Y. Niibori, Complex formation of Eu(III) with humic acid and polyacrylic acid, *Radiochim. Acta* 90 (2002) 594–574.

[17] M.U. Kumke, S. Eidner, T. Krüger, Fluorescence quenching and luminescence sensitization in complexes of  $Tb^{3+}$  and  $Eu^{3+}$  with humic substances, *Environ. Sci. Technol.* 39 (2005) 9528–9533.

[18] E. Tipping, *Cation Binding by Humic Substances*, Cambridge University Press, New York, 2002.

[19] A.W. Underdown, C.H. Langford, Light scattering of a polydisperse fulvic acid, *Anal. Chem.* 53 (1981) 2139–2140.

[20] N.M. Thang, H. Geckeis, J.I. Kim, H.P. Beck, Application of the flow field flow fractionation (FFFF) to the characterization of aquatic humic colloids: evaluation and optimization of the method, *Colloid Surface A.* 181 (2001) 289–301.

- [21] T. Takahashi, H. Kawashima, H. Sugisawa, T. Baba,  $^{207}\text{Pb}$  chemical shift thermometer at high temperature for magic angle spinning experiments, *Solid State Nucl. Magn. Reson.* 15 (1999) 119–123.
- [22] A.C. Kunwar, G.L. Turner, E. Oldfield, Solid-state spin-echo Fourier transform NMR of  $^{39}\text{K}$  and  $^{67}\text{Zn}$  salts at high field, *J. Magn. Reson.* 69 (1986) 124–127.
- [23] A.E. Bennett, C.M. Rienstra, M. Auger, K.V. Lakshmi, R.G. Griffin, Heteronuclear decoupling in rotating solids, *J. Chem. Phys.* 103 (1995) 6951–6958.
- [24] M.F. Czarniecki, E.R. Thornton,  $^{13}\text{C}$  NMR chemical shift titration of metal ion-carbohydrate complexes. An unexpected dichotomy for  $\text{Ca}^{+2}$  binding between anomeric derivatives of *N*-acetylneuraminic acid, *Biochem. Biophys. Res. Commun.* 74 (1977) 553–558.
- [25] P.W. Jolly, R. Mynott, The application of  $^{13}\text{C}$ -NMR spectroscopy to organo-transition metal complexes, *Adv. Organomet. Chem.* 19 (1981) 257–304.
- [26] M.E. Bjornson, D.C. Corson, B.D. Sykes,  $^{13}\text{C}$  and  $^{113}\text{Cd}$  NMR studies of the chelation of metal ions by the calcium binding protein parvalbumin, *J. Inorg. Biochem.* 25 (1985) 141–149.
- [27] M. Kalinowska, R. Świsłocka, W. Lewandowski, Zn(II), Cd(II) and Hg(I) complexes of cinnamic acid: FT-IR, FT-Raman,  $^1\text{H}$  and  $^{13}\text{C}$  NMR studies, *J. Mol. Struct.* 993 (2011) 404–409.
- [28] E.J.W. Verwey, J.Th.G. Overbeek, *Theory of the Stability of Lyophobic Colloids*, Dover Publications, New York, 1948.
- [29] J. Israelachvili, *Intermolecular and Surface Forces*, Academic Press, Amsterdam, 1991.
- [30] I. Christl, R. Kretschmar, C-1s NEXAFS spectroscopy reveals chemical fractionation of humic acid by cation-induced coagulation, *Environ. Sci. Technol.* 41 (2007) 1915–1920.

- [31] L. Rao, G.R. Choppin, Thermodynamic study of the complexation of neptunium (V) with humic acids, *Radiochim. Acta* 69 (1995) 87–95.
- [32] M. Kawahigashi, N. Fujitake, T. Takahasi, Structural information obtained from spectral analysis (UV-VIS, IR,  $^1\text{H}$  NMR) of particle size fractions in two humic acids, *Soil Sci. Plant Nutr.* 42 (1996) 355–360.
- [33] G.R. Choppin, P.M. Shanbhag, Binding of calcium by humic acid, *J. Inorg. Nucl. Chem.* 43 (1981) 921–922.
- [34] F.J. Sikora, F.J. Stevenson, Silver complexation by humic substances: conditional stability constants and nature of reactive sites, *Geoderma* 42 (1988) 353–363.
- [35] P. D. Hancock, F. Marsicano, Parametric correlation of formation constants in aqueous solution. 1. Ligand with small donor atoms, *Inorg. Chem.* 17 (1978) 560–564.
- [36] L. Marang, P.E. Reiller, S. Eidner, M.U. Kumke, M.F. Benedetti, Combining spectroscopic and potentiometric approaches to characterize competitive binding to humic substances, *Environ. Sci. Technol.* 42 (2008) 5094–5098.
- [37] L. Marang, S. Eidner, M.U. Kumke, M.F. Benedetti, P.E. Reiller, Spectroscopic characterization of the competitive binding of Eu(III), Ca(II), and Cu(II) to a sedimentary originated humic acid, *Chem. Geol.* 264 (2009) 154–161.
- [38] M. Plaschke, J. Rothe, M.A. Denecke, T. Fanghänel, Soft X-ray spectromicroscopy of humic acid europium(III) complexation by comparison to model substances, *J. Electron Spectrosc. Relat. Phenom.* 135 (2004) 53–62.
- [39] R.R. Engebretson, R.von Wandruszka, Microorganization in dissolved humic acids, *Environ. Sci. Technol.* 28 (1994) 1934–1941.
- [40] R.R. Engebretson, T. Amos, R.von Wandruszka, Quantitative approach to humic acid associations, *Environ. Sci. Technol.* 30 (1996) 990–997.

[41] J. Novák, J. Kozler, P. Janoš, J. Čežíková, V. Tokarová, Humic acids from coals of the North-Bohemian coal field I. Preparation and characterization, *React. Funct. Polym.* 47 (2001) 101–109.

[42] J.D. Ritchie, E.M. Perdue, Proton-binding study of standard and reference fulvic acids, humic acids, and natural organic matter, *Geochim. Cosmochim. Acta* 67 (2003) 85–96.

**Table 1**

Ash and acid contents of HAs.

	Ash (%)	Acid content (meq g <sup>-1</sup> ) <sup>a</sup>	
		-COOH	Total acidity
Fluka HA	16.07 <sup>b</sup>	0.84 (1.01) <sup>b</sup>	6.26 (7.46) <sup>b</sup>
IHSS peat HA	1.72 <sup>c</sup>	4.95 (5.04) <sup>d</sup>	6.09 (6.20) <sup>d</sup>

<sup>a</sup> Values of acid content in parentheses are from ash-free samples

<sup>b</sup> Novák et al. [41]

<sup>c</sup> Huffman Laboratories, Wheat Ridge, CO, USA,

<http://www.humicsubstances.org/elements.html>

<sup>d</sup> Ritchie and Perdue [42]

**Table 2**

Debye lengths under solution conditions where there is a significant absorbance reduction (>50%).

	Debye length (nm)			
	Na(I)	Ag(I)	Ca(II)	Eu(III)
Fluka HA	0.22	2.91	2.50	19.2
IHSS peat HA	0.16	2.68	2.28	17.6

In the calculations, metal ions were assumed to be in their free unbound state. The Debye length for Na(I), in the case of IHSS HA, was calculated at the maximum Na(I) concentration ( $3.5 \text{ mol L}^{-1}$ ), where the absorbance was reduced by less than 50%.

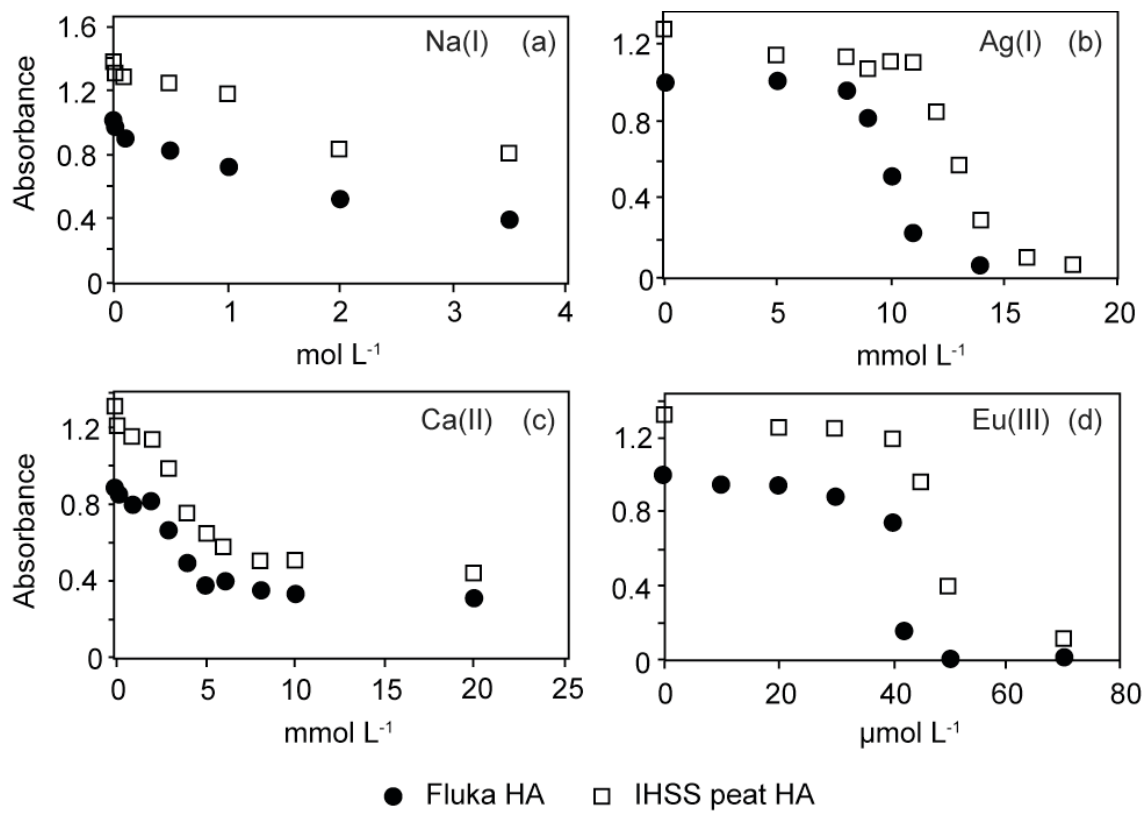


**Fig. 1**

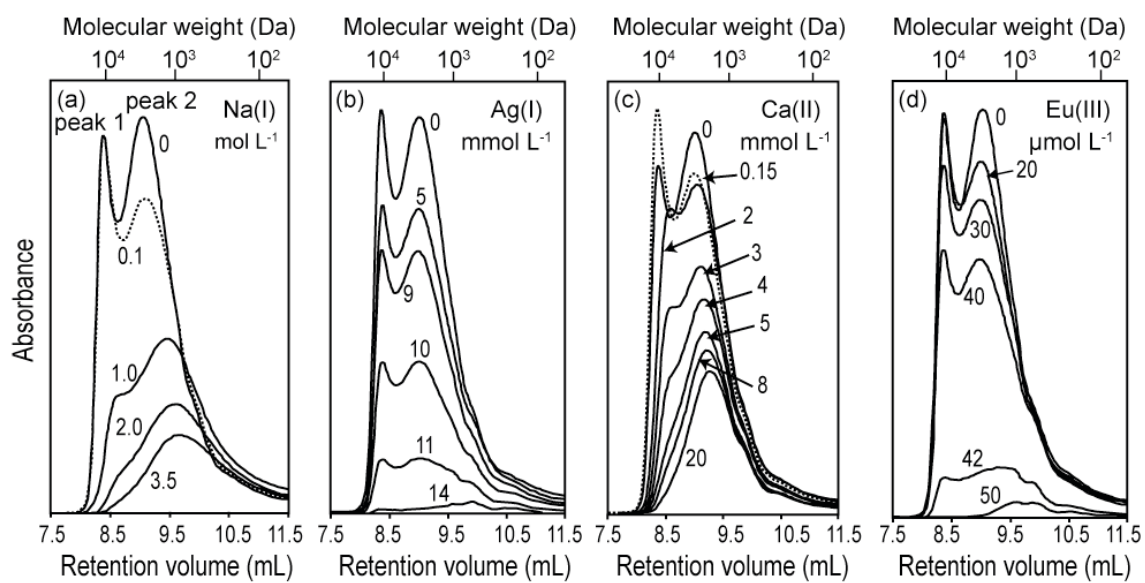


**Fig. 2**

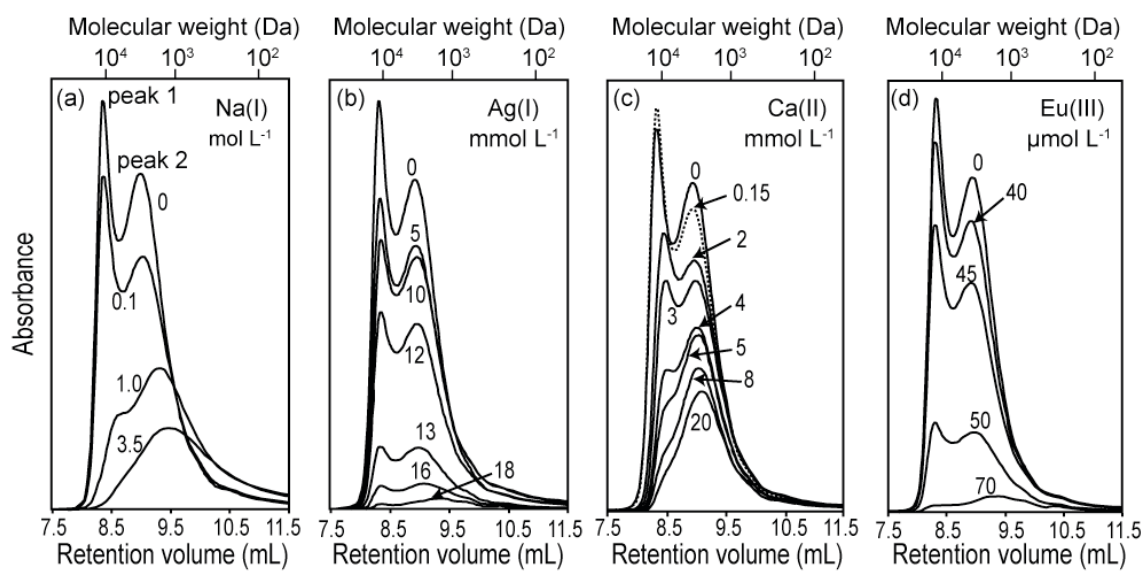


**Fig. 3**

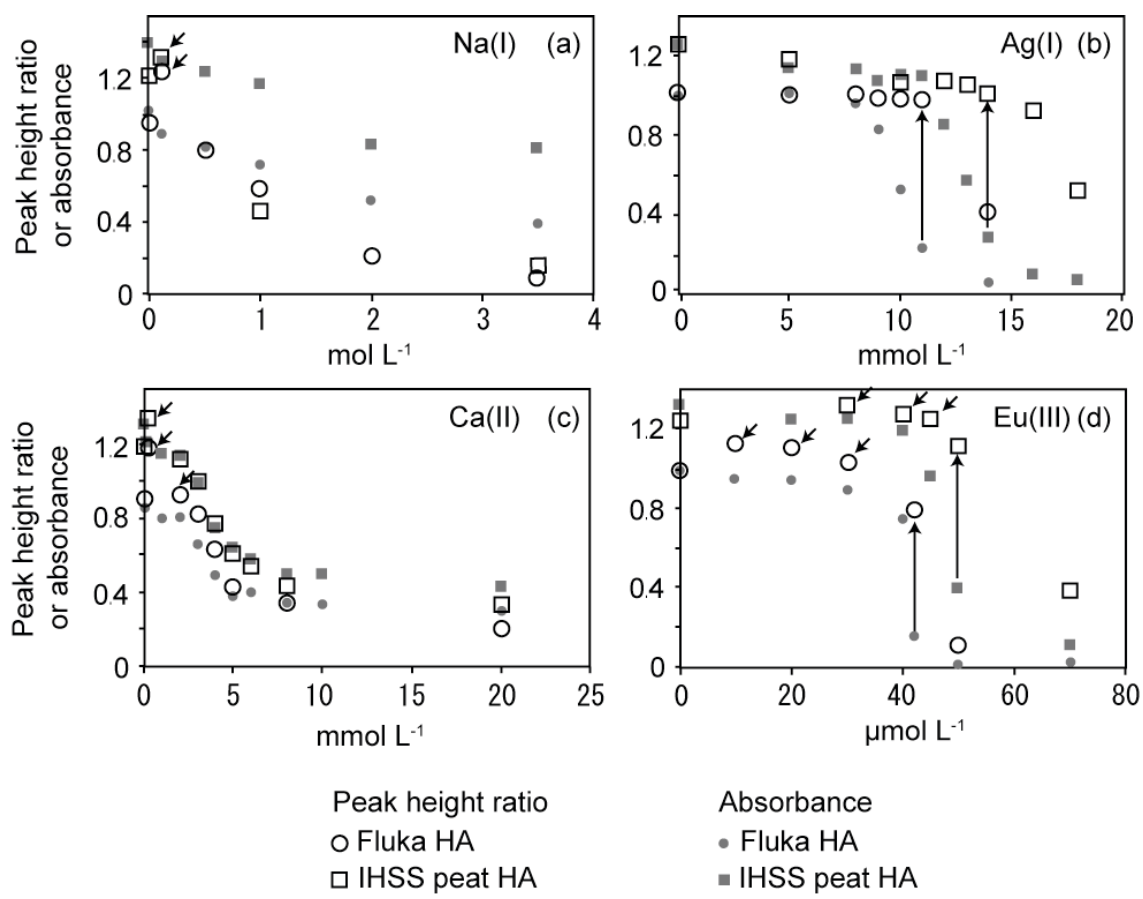


**Fig. 4**

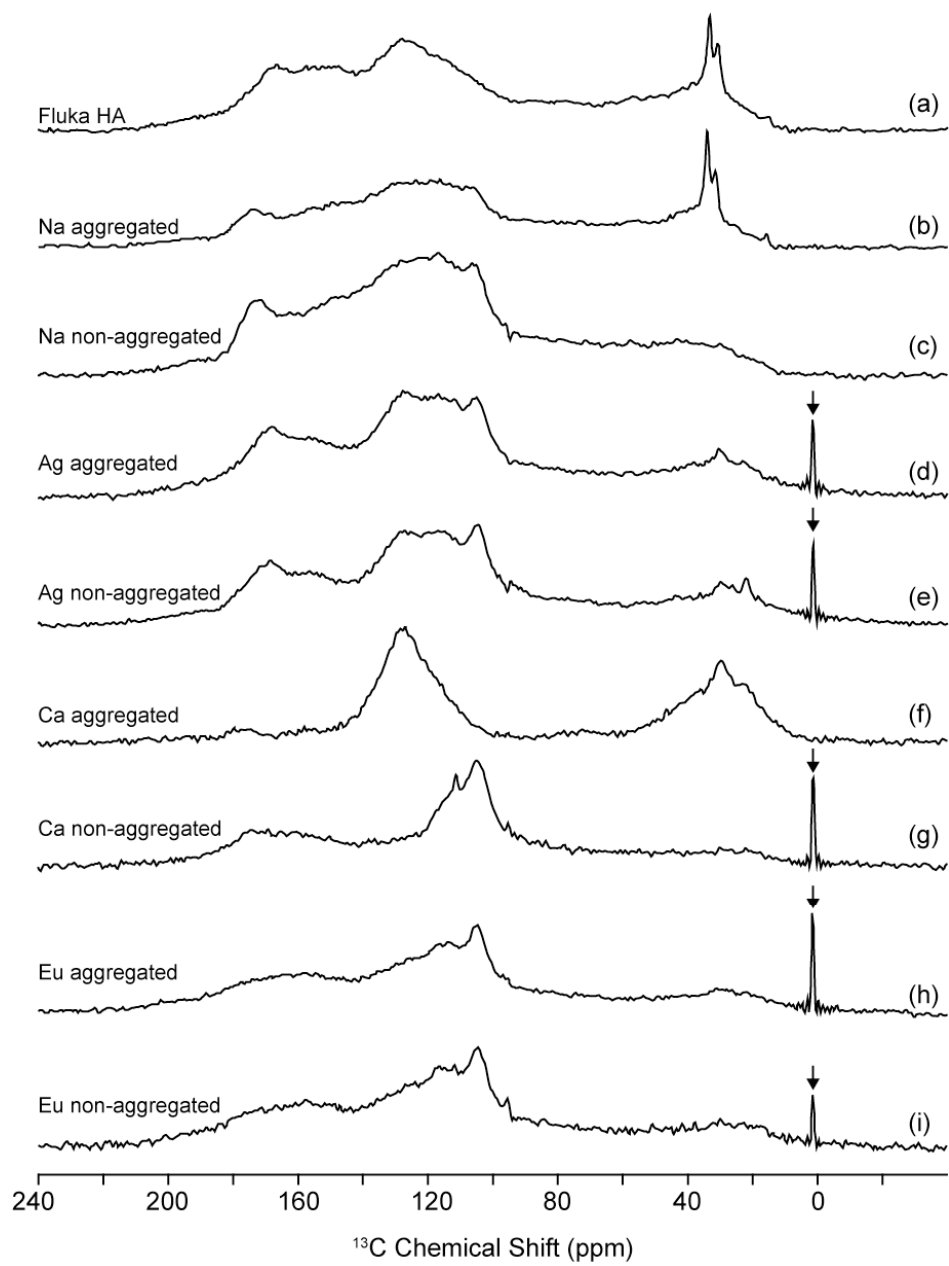


**Fig. 5**